Antiviral Research 82 (2009) 122–133

Contents lists available at ScienceDirect

Antiviral Research

journal homepage: www.elsevier.com/locate/antiviral

Inhibition of Japanese encephalitis virus replication by peptide nucleic acids targeting *cis*-acting elements on the plus- and minus-strands of viral RNA

Ji-Seung Yoo, Chan-Mi Kim, Jung-Hee Kim, Jee-Yon Kim, Jong-Won Oh*

Department of Biotechnology, Yonsei University, 134 Shinchon-dong, Seodaemun-gu, Seoul 120-749, Republic of Korea

ARTICLE INFO

Article history:
Received 22 October 2008
Received in revised form 12 January 2009
Accepted 9 February 2009

Keywords:
JEV
Peptide nucleic acids (PNAs)
Antisense
RdRp
cis-Acting element

ABSTRACT

Japanese encephalitis virus (JEV) is a major cause of acute viral encephalitis in humans. The single-stranded, plus-sense viral genome, which is used for translation and minus-strand RNA synthesis, and its complementary minus-strand viral RNA contain various sequences and RNA secondary structures conserved in flaviviruses, providing potential targets for antisense agents. Here, we investigated the antiviral effects of peptide nucleic acids (PNAs) targeting *cis*-acting signals at the 5′-untranslated region (UTR), 3′-UTR, and genome cyclization motifs on the plus-strand RNA, as well as the 95-nucleotide 3′-end of the minus-strand RNA, which serves as a template for plus-strand RNA synthesis by the viral RNA-dependent RNA polymerase (RdRp). Among the tested cell-penetrating peptide (CPP)–PNA conjugates, a 17-mer PNA conjugate targeting the top of the 3′-UTR loop structure was most effective in suppressing virus proliferation. *In vitro* RdRp assays and electrophoretic mobility shift assays using a functional recombinant JEV RdRp showed that the 3′-terminal region-targeting PNAs could inhibit RNA synthesis by competing with viral RdRp for binding to a selected *cis*-acting element at the 3′-end of plus- and minus-strand viral RNAs. Collectively, our results suggest that CPP–PNA conjugates can suppress JEV proliferation by blocking RNA–protein or RNA–RNA interactions essential for productive viral infection.

1. Introduction

Japanese encephalitis virus (JEV) is the most common cause of epidemic viral encephalitis worldwide, with approximately 35,000–50,000 cases and 10,000 deaths annually (Tsai, 2000). JEV is a member of genus *Flavivirus* in the family *Flaviviridae*, and is transmitted between vertebrate hosts by mosquitoes. Other emerging pathogens in the *Flavivirus* genus include dengue virus (DENV), yellow fever virus (YFV), West Nile virus (WNV), Kunjin virus (KUNV), and Murray Valley encephalitis virus (MVEV) (Lindenbach and Rice, 2003). JEV is widely distributed in Asia, including Japan, China, Taiwan, Korea, Philippines, the far-eastern region of the former Soviet Union, all of Southeast Asia, and India (Solomon, 2003). The recent outbreaks of JEV and other emerging and re-emerging flaviviruses have made the prevention and treatment of flavivirus infections a global public health priority (Mackenzie et al., 2004; Parida et al., 2006). However, currently no specific, effective antiviral drugs are available for the treatment of JEV infection (Leyssen et al., 2000, 2003; Shi, 2002).

The genome of JEV is a single-stranded, plus-sense RNA approximately 11 kb in length, which has a single open reading frame (ORF) flanked by 5′- and 3′-untranslated regions (UTRs) containing *cis*-acting elements required for viral RNA translation and replication (Sumiyoshi et al., 1987; Chambers et al., 1990; Markoff, 2003). The single large ORF encodes a polyprotein of ~3400 amino acids that is subsequently processed by both host and viral proteases into three structural proteins and seven nonstructural (NS) proteins (Chambers et al., 1990). Among the seven NS proteins, the methyltransferase and RNA-dependent RNA polymerase (RdRp) NS5 is a key viral enzyme essential for viral RNA replication (Lindenbach and Rice, 2003; Kim et al., 2007).

Antisense oligonucleotides and small interfering RNA (siRNA) molecules have been demonstrated to be effective in inhibiting replication of various pathogenic RNA viruses (Spurgers et al., 2008; Stein and Shi, 2008). For flaviviruses, a modified antisense oligonucleotide, phosphorodiamidate morpholino oligomer (PMO) has been used to significantly reduce titers of WNV and JEV in cell cultures (Deas et al., 2007). Intracranial administration of lentivirus-mediated delivery of short hairpin RNA or lipid-complexed siRNA has also been used for protection against lethal encephalitis in mice infected with neurotropic flaviviruses, JEV and WNV (Kumar et al., 2006). Antisense peptide nucleic acid (PNA) is a synthetic nucleic acid derivative with a noncyclic peptide-like backbone with side chains containing the heterocyclic bases found in nucleic acids (Nielsen et al., 1991). The polyamide PNA backbone is flexible and neutral, imposing distances between the nucleobases that are similar to those found in natural DNA and RNA. Owing to its good hybridization properties such as high binding affinity

* Corresponding author. Tel.: +82 2 2123 2881; fax: +82 2 362 7265.
E-mail address: jwoh@yonsei.ac.kr (J.-W. Oh).

0166-3542/$ – see front matter © 2009 Elsevier B.V. All rights reserved.
doi:10.1016/j.antiviral.2009.02.187

and improved sequence specificity, and high biostability, PNA has promise as a candidate sequence-specific antiviral drug (Lundin et al., 2006).

In the present study, we designed various antisense PNAs targeting *cis*-acting elements at the plus- and minus-strands of JEV RNA, which were identified by performing a comparative analysis of functionally characterized flavivirus sequences and structures. The antiviral activities of the PNAs were investigated in virus-infected cells by the delivery of individual PNAs conjugated to a cell-penetrating human immunodeficiency virus (HIV)-1 Tat peptide. We identified various *cis*-acting signals on the plus- and minus-strands of JEV viral RNA that can be assessed for their sensitivity to sequence-specific antisense Tat–PNA conjugates. Our results demonstrated that interference with viral RNA long-range interaction or viral RdRp binding to the 3′-end region of plus- and minus-strands of viral RNAs by PNAs could effectively suppress productive viral infections.

2. Materials and methods

2.1. Cell culture and virus

Baby hamster kidney (BHK)-21 cells were maintained in Dulbecco's minimal essential medium (DMEM; Bio Whittaker) supplemented with 10% fetal bovine serum (FBS; Invitrogen) and 1% penicillin/streptomycin sulfate (Invitrogen) at 37 °C in 5% CO_2. The Nakayama strain of JEV (Kim et al., 2007) was used for the infection of BHK-21 cells.

2.2. Genome and secondary structure analysis

Various flavivirus complete genome sequences were obtained from the public database on the Entrez server at NCBI (http://www.ncbi.nlm.nih.gov) and sequence alignment searches were performed using the Align X program, a component of the Vector NTI suite (Informax). Conserved motifs and domains of flavivirus were scanned online using Biology WorkBench 3.2 (http://workbench.sdsc.edu/). RNA secondary structures were predicted by using the Mfold program (Zuker, 2003). The RNA structure drawings were edited and annotated using Adobe illustrator.

2.3. PNA design and synthesis

All PNAs and PNA derivatives were obtained from Panagene Inc. (Daejeon, Korea). PNAs were synthesized using benzothiazole-2-sulfonyl PNA monomers. For efficient cellular uptake, the HIV-1 Tat peptide $Tat_{48–60}$ (GRKKRRQRRRPPQ) (Suzuki et al., 2002; Zhao and Weissleder, 2004) or $Tat_{57–49}$ (RRRQRRKKR) (Wender et al., 2000) was covalently linked to the N-terminus of the PNA via an O-linker (AEEA, 8-amino-3,5-dioxo-octanic acid). For labeling of PNAs, 6-carboxyfluorescein (FAM) was covalently linked to the N-terminus. PNAs were purified by reverse phase high-performance liquid chromatography using a C-18 column, and their purity was confirmed by matrix-assisted laser desorption ionization time of flight mass spectrometry. PNA targets were screened with BLAST (http://www.ncbi.nlm.nih.gov/BLAST/) against known human mRNA sequences in order to avoid unintentional gene-silencing effects.

2.4. Antiviral activity

BHK-21 cells were seeded in 6-well or 12-well plates and grown in complete DMEM containing 10% FBS and 1% penicillin/streptomycin at 37 °C. Cells were then infected with JEV at a multiplicity of infection (MOI) of 0.05 by adsorption for 90 min. After the removal of unbound virus, infected cells were incubated for 5 h with the indicated Tat-conjugated PNAs dissolved in serum-free DMEM. After PNA uptake, cells were washed with serum-free DMEM and further incubated in fresh complete DMEM at 37 °C. Culture supernatants were then collected at 48 h post-infection (PI), and virus titers were determined using plaque assays. Cells were also harvested for the analyses of JEV RNA copy number and protein levels by real-time RT-PCR and Western blot analysis, respectively.

2.5. MTT assay

Cell viability following PNA treatment was determined by the conversion of thiazolyl blue, 3-(4,5-dimethylthiazol-2-yl)-2,5-diphenyl tetrazolium bromide (MTT), to blue formazan crystals. Approximately 2×10^4 BHK-21 cells seeded into a 96-well plate were incubated with different concentrations of Tat–PNA conjugates for 5 h. Cells were then maintained in DMEM containing 10% FBS for 48 h. Thereafter, 50 μl of MTT (Sigma–Aldrich) solution (2 mg/ml) was added to the culture medium and plates were incubated for 4 h at 37 °C. Formazan crystals were dissolved in 500 μl dimethyl sulfoxide (Sigma–Aldrich), and the optical density at 560 nm was read on a 96-well microplate autoreader (FLUOstar OPTIMA, BMG Lab Technologies). Results were expressed relative to the optical density of wells containing control (untreated) cells, defined as 100% viability. Assays were performed in triplicate.

2.6. Plaque assay

Confluent BHK-21 cells in 6-well plates were adsorbed with various dilutions of viral culture supernatants for 90 min at 37 °C in a 5% CO_2 incubator. After adsorption, unbound virus was removed, and cells were washed with serum-free DMEM twice. Cells were then overlaid with 3 ml of solid culture medium (5% FBS, 1% low melting agarose, 1× DMEM, 1% penicillin/streptomycin). After incubation for 48 h, plates were overlaid with 1.5 ml of solid medium [5% FBS, 1% low melting agarose, 1× DMEM, 1% penicillin/streptomycin, 0.05% neutral red (Sigma–Aldrich)]. After incubation for 12 h at 37 °C, plaques were counted.

2.7. Real-time quantitative reverse transcription-PCR

Total RNA from JEV-infected BHK-21 cells was extracted with TRIzol reagent (Invitrogen) and purified according to the Manufacturer's recommendations. Intracellular JEV genome levels were quantified with the DyNAmo Probe 2-step qRT-PCR kit (Finnzymes) and a CHROMO4 Continuous Fluorescence Detector (MJ Research). For cDNA preparation, total RNA (1 μg) was reverse transcribed with the antisense primer 5′-ATTCCCAGGTGTCAATATGCTGTT-3′. Triplicate cDNA samples were amplified with the qRT-PCR kit. The primer and probe sequences specific for the JEV 3′-UTR were as follows: sense primer, 5′-GGTGTAAGGACTAGAGGTTAGAGG-3′; antisense primer, 5′-ATTCCCAGGTGTCAATATGCTGTT-3′; and a dual fluorophore-labeled probe, 5′-FAM (6-carboxyfluorescein)-CCCG-TGGAAACAAAAAAATGCGGC-TAMRA (6-carboxytetramethylrhodamine)-3′. Cellular glyceraldehyde-3-phosphate dehydrogenase (GAPDH) mRNA from the same RNA extract was used as an internal control. An RNA standard (JEV 3′-UTR) was prepared by *in vitro* transcription with T7 RNA polymerase and purified by electrophoresis on a 5% polyacrylamide gel containing 8 M urea as described previously (Oh et al., 2000).

2.8. Fluorescence microscopy

BHK-21 cells grown in a cover-glass bottom culture dish were incubated with FAM-labeled $Tat_{57–49}$-conjugated PNA J3U4 (2 μM, Table 1) for 1 min in serum-free DMEM. Cells were then washed

Table 1
PNAs used in this study.

Name[a]	N-terminal HIV Tat sequence	Sequence (5′ → 3′)[b]	Target region[c]	Length (mer)
J5U1	H-RRRQRRKKR	AAGTTCACACAGATA	8–22	15
J4U2	H-RRRQRRKKR	ACGATACTAAGCCAA	24–38	15
J5C1	H-RRRQRRKKR	CATATTGATGGCCCG	129–143	15
J5C2	H-RRRQRRKKR	CGTTTCAGCATATTG	145–151	15
J3C1	H-RRRQRRKKR	TTCCCAGGTGTCAAT	10,867–10,881	15
J3C2	H-RRRQRRKKR	CCCAGGTGTCAATAT	10,869–10,883	15
J3U1	H-RRRQRRKKR	GGCGCTCTGTGCC	10,930–10,942	13
J3U2	H-RRRQRRKKR	TCGGCGCTCTGTGCC	10,928–10,942	15
J3U3	H-RRRQRRKKR	CTTCGGCGCTCTGTGCC	10,926–10,942	17
J3U4	H-RRRQRRKKR	ACATACTTCGGCG	10,931–10,943	13
J3U5	H-RRRQRRKKR	ACATACTTCGGCGCT	10,931–10,945	15
J3U6	H-RRRQRRKKR	ACATACTTCGGCGCTCT	10,931–10,947	17
J3U4-1	H-GRKKRRQRRRPPQ	ACATACTTCGGCG	42–55	13
J3U4-1M1	H-GRKKRRQRRRPPQ	ACATA***G***TTCGGCG	42–55	13
J3U4-1M2	H-GRKKRRQRRRPPQ	ACATA***G***TT***G***GGCG	42–55	13
HCV-X	H-GRKKRRQRRRPPQ	CGGACCTTTCACA	HCV-X-tail	13
J3U3(−)[d]	H-RRRQRRKKR	GCTTAGTATCGTTGAGA	(−) 10,957–10,973	17
J3U4(−)	H-RRRQRRKKR	AGTTTATCTGTGTGAAC	(−) 10,934–10,950	17
fJ3U1(−)	–	TTAGAACGGAAGATAAC	(−) 10,900–10,916	17
fJ3U2(−)	–	GCAGTTTAAACAGTTTT	(−) 10,899–10,882	17
fJ3U3(−)	–	GCTTAGTATCGTTGAGA	(−) 10,900–10,916	17
fJ3U4(−)	–	AGTTTATCTGTGTGAAC	(−) 10,899–10,882	17
fJ3U4	–	ACATACTTCGGCG	10,931–10,943	13

[a] PNAs are listed from N- to C-terminus, which correspond to the 5′- and 3′-terminus in nucleic acids, respectively.
[b] Underlined boldface letters indicate mismatched bases.
[c] Nucleotide of target regions corresponds to the published JEV genome sequence (GenBank: NC_001437).
[d] (−) indicates minus-strand JEV RNA.

twice with PBS and complete medium was added. Fluorescence was detected using a Zeiss LSM 510 META confocal microscope.

2.9. Western blot analysis

Cell lysates were separated by 10% SDS-PAGE and transferred to a nitrocellulose Hybond ECL membrane (GE Healthcare Life Sciences) in a Trans-Blot SD semidry transfer cell (Bio-Rad). The membrane was blocked with 5% BSA in TBST buffer (20 mM Tris–HCl [pH 7.4], 150 mM NaCl, 0.1% Tween 20), then probed with anti-JEV NS5 antibody, anti-envelope antibody, or anti-tubulin antibody (Santa Cruz Biotechnology) as described previously (Kim et al., 2007). Bound antibody was detected using peroxidase-conjugated secondary antibodies, and visualized using enhanced chemiluminescence (ECL; GE Healthcare Life Sciences).

2.10. Expression and purification of recombinant JEV NS5 protein from E. coli

JEV NS5 protein was expressed in *E. coli* TOP10 cells (Invitrogen) transformed with pTrcHisB-JEVNS5 (Kim et al., 2007). NS5 protein was expressed at 18 °C for 12 h by the addition of 1 mM isopropyl-β-D-thiogalactopyranoside (IPTG). The NS5 protein was purified by metal affinity chromatography using Ni-nitrilotriacetic acid (NTA)-agarose (Qiagen) resin as described previously (Kim et al., 2007), followed by affinity chromatography using a heparin-Sepharose column (GE Healthcare Life Sciences) as described previously (Kim et al., 2004). Protein concentration was determined using a Bio-Rad protein assay kit with bovine serum albumin as a standard.

2.11. Preparation of in vitro transcripts

The DNA templates for the 83-nt RNA template (representing the 83-nt RNA from the 3′-end of the JEV genome) and the c5′-UTR (representing the region complementary to the 5′-UTR of the JEV genome) were obtained by PCR with Vent DNA polymerase (New England Biolabs) and the specific primers using pBAC^{SP6}/JVFLx/XbaI (Yun et al., 2003) as a template, as previously described (Kim et al., 2004). For the preparation of the c5′-UTR full-length and deletion derivatives c5′-UTRΔ24, c5′-UTRΔ46, and c5′-UTRΔ67, DNA templates were obtained by PCR with the reverse primers (5′-TAATACGACTCACTATA***GGTTATCTTCCGTTCTAA***-3′), (5′-TAATACGACTCACTATA***GTTTAAACTGCACTAATC***-3′), (5′-TAATACGACTCACTATA***GATTCTTCTCAACGATAC***-3′), and (5′-TAATACGACTCACTATA***GCCAAGAAGTTCACACAG***-3′), respectively, in combination with a forward primer (5′-***AGAAGTTTATCTGTGTG***-3′). The T7 RNA polymerase promoter sequence is underlined and the sequence complementary to the DNA template sequence is shown in boldface italic. The PCR-amplified DNA products were gel-purified and used for *in vitro* transcription using the T7 MEGAscript kit (Ambion) according to the Manufacturer's instructions. For the generation of ^{32}P-labeled RNA probes, *in vitro* transcription was performed using an rNTP mixture containing 7.5 mM each of ATP, GTP, CTP, and 0.15 mM UTP, and 20 μCi of [α-^{32}P]UTP. All of the *in vitro* transcribed RNAs were gel-purified as described previously (Kim et al., 2007).

2.12. RNA-dependent RNA polymerase activity assay

In vitro RdRp activity assays were performed with 200 ng of purified JEV NS5 in a total volume of 25 μl RdRp reaction buffer (50 mM Tris–HCl [pH 8.0], 50 mM NaCl, 2.5 mM $MnCl_2$, 25 mM potassium glutamate, 1 mM DTT, 10% glycerol, 20 units of RNase inhibitor [Promega]) containing cold ribonucleotide mixture (0.5 mM each ATP, CTP, and GTP, and 5 μM UTP) and 10 μCi of [α-^{32}P]UTP (3000 Ci/mmol; GE Healthcare Life Sciences). The reaction mixture was incubated with 200 ng of RNA template for 2 h at 30 °C. RdRp reaction products were processed and resolved on an 8 M urea–8% polyacrylamide gel, as previously described (Kim et al., 2007). After electrophoresis, gels were stained with ethidium bromide to locate the template positions, dried, and exposed to X-ray film for autoradiography.

2.13. Gel electrophoretic mobility shift assay

For the analysis of PNA–RNA and RNA–protein interactions, a ^{32}P-labeled c5′-UTR 95-nt RNA probe (50 fmol; 5000 cpm) was

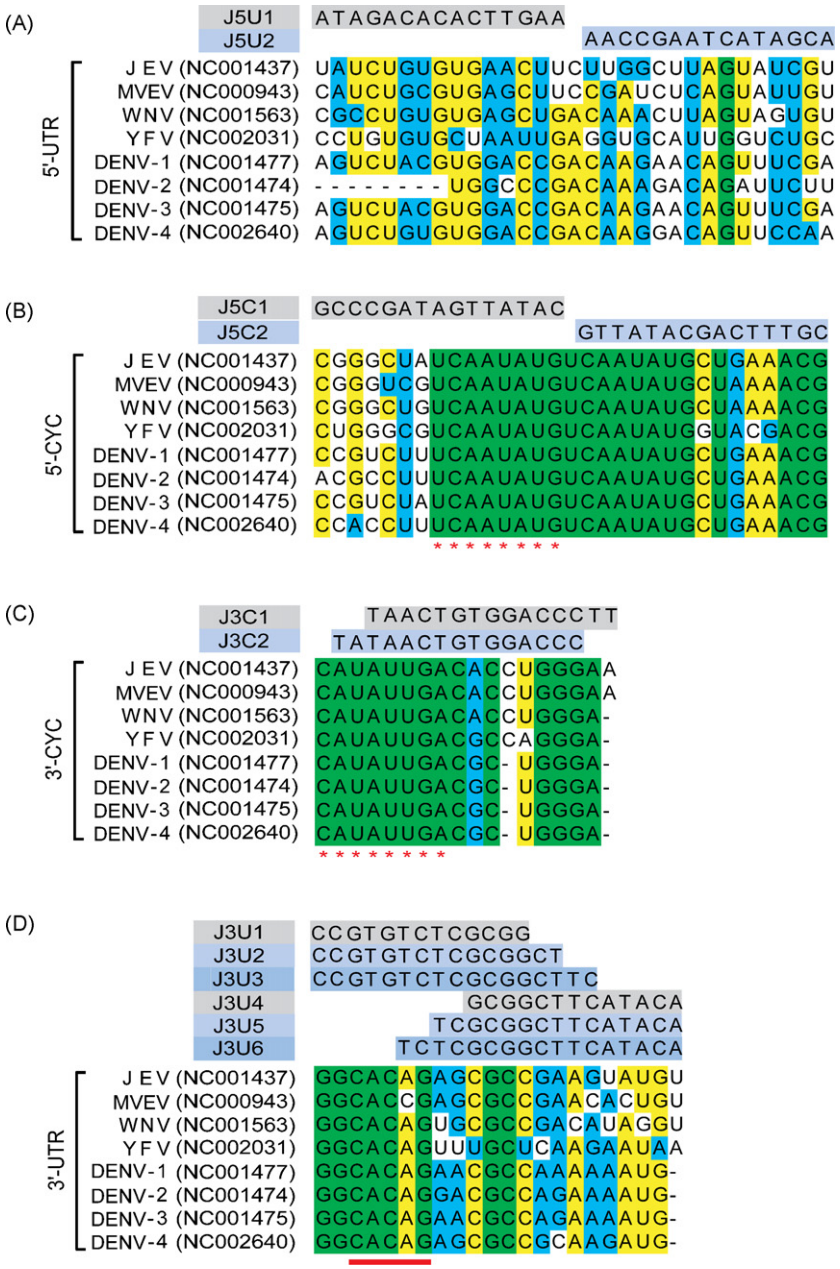

Fig. 1. Alignment of the conserved sequences of selected flavivirus genomes and the antisense sequences of PNAs targeting the JEV genome. The NCBI Entrez accession numbers of the aligned sequences are NC001437, JEV; NC000943, Murray valley encephalitis virus (MVEV); NC001563, West Nile virus (WNV); NC002031, yellow fever virus (YFV); NC001477, dengue virus serotype 1 (DENV-1); NC001474, dengue virus serotype 2 (DENV-2); NC001475, dengue virus serotype 3 (DENV-3); and NC002640, dengue virus serotype 4 (DENV-4). The viral genomic sense sequences are written 5′–3′. Completely conserved motifs, identical residues, and similar residues are colored in green, yellow, and blue, respectively. Dashes indicate gaps introduced in the sequence for optimal alignment. Red asterisks indicate the conserved 8-nt sequences in the 5′ and 3′ cyclization motifs, which are complementary to each other. The conserved penta-nucleotide region in the 3′-UTR is underlined in red. PNAs were targeted to *cis*-acting elements of the JEV genome that are well-conserved in flaviviruses (see Table 1 for the target region of each PNA). The antisense sequences of each PNA are written 3′–5′ above the genome sequences they target.

incubated with various concentrations of PNA in a total volume of 10 μl of the RdRp reaction buffer. After incubation at 4 °C for 30 min, an equal volume of non-denaturing loading buffer (100% glycerol, 0.02% each xylene cyanol and bromophenol blue) was added to the reaction mixtures, which were then resolved by electrophoresis on a 5% non-denaturing polyacrylamide gel, in 0.5× Tris–borate–EDTA buffer (45 mM Tris base, 45 mM H_3BO_3, 1 mM EDTA) at a constant voltage of 120 V at 4 °C. After electrophoresis, the gel was dried and exposed to X-ray film for autoradiography.

3. Results

3.1. Comparative analysis of cis-acting elements in the JEV genome for the determination of PNA-targeting sites

The plus-strand RNA genome of JEV acts as mRNA as well as a template for minus-strand viral RNA synthesis. So far, only a few individual *cis*-acting elements in the JEV genome have been identified experimentally. Therefore, we searched for potentially important *cis*-acting elements that can be targeted by antisense

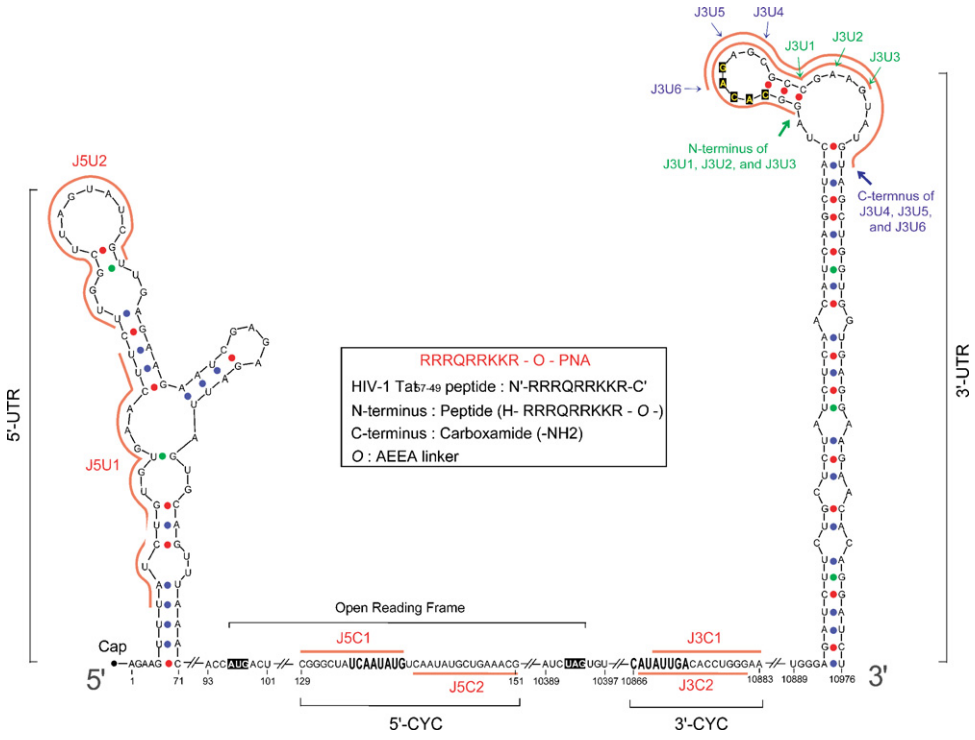

Fig. 2. RNA secondary structures and sequences targeted by PNAs. The RNA secondary structure, predicted using Mfold, for the 5′- and 3′-UTRs of the JEV genome, and the sequences of potential genome cyclization (CYC) motifs are shown as well as the PNA-targeting sites, which are indicated with red lines. The perfect 8-nt complementary sequences for long-range cross-talk between the 5′- and 3′-CYC motifs are shown in bold. The 3′-UTR penta-nucleotide sequence and translation initiation and termination codons of the long open reading frame are shadowed in black. The positions of N- and C-termini of the indicated PNAs targeting the top of the 3′-UTR loop structure are marked with arrows.

PNAs by aligning the JEV genome with the functionally important 5′- and 3′-UTRs and the genome cyclization motifs previously found in other related flaviviruses. The 5′-UTR of JEV is not well-conserved in nucleotide sequence with other flaviviruses (Fig. 1) (Markoff, 2003), but it is predicted to form a conserved secondary structure that was also found in other flaviviruses (Fig. 2) (Thurner et al., 2004). This region has been shown to play an important role in translation and/or replication as demonstrated for DENV by a reverse genetics approach using an infectious cDNA clone (Cahour et al., 1995). The 3′-UTR of the JEV genome also forms a highly conserved stem-loop (SL) structure (Fig. 2) that is also proposed for other flavivirus genomes (Proutski et al., 1997; Markoff, 2003), even though the linear sequence of the 3′-UTR is only partially conserved among different flaviviruses (Fig. 1). The 3′-UTR is functionally conserved among many plus-strand RNA viruses in that it plays a role in the regulation of translation and RNA stability in a manner typical for cellular mRNA (Decker and Parker, 1995). However, the most significant function of the 3′-UTR is as a site for the initiation of minus-strand synthesis (Dreher, 1999), and we previously demonstrated this for JEV (Kim et al., 2007). Like all mosquito-borne flaviviruses, the JEV 3′-UTR has the conserved penta-nucleotide 5′-CACAG-3′ in an unpaired region, forming a closed loop within the conserved SL structure (Figs. 1 and 2) (Hahn et al., 1987). The function of this conserved sequence in JEV and other flaviviruses is unknown. Like other flaviviral genomes, the JEV genome may form a panhandle-like structure by the hybridization of the two conserved complementary sequences at the 5′- and 3′-cyclization motifs (CYC) (Fig. 1). The 8-nt conserved sequence (5′-UCAAUAUG-3′) at the 5′-CYC located at the region encoding the capsid protein is exactly complementary to the conserved matching sequence (5′-CAUAUUGA-3′) at the 3′-CYC. Base-pairing between these regions can lead to cyclization of the viral genome, which may be important for the regulation of genome translation, replication, or packaging (Hahn et al., 1987; Brinton and Dispoto, 1988; Khromykh et al., 2001; You et al., 2001).

3.2. *Cell-based evaluation of anti-JEV effects of various Tat–PNA conjugates targeting cis-acting elements on the plus-strand viral genome*

The *cis*-acting elements described above are likely the sites to which host and/or viral proteins bind or with which RNA–RNA interaction occurs for viral genome expression and RNA synthesis, and thus represent potential antisense targets for controlling JEV infection. For an initial test of the anti-JEV effects of PNAs, we first designed various 15-mer antisense PNAs to target highly conserved RNA structures at the 5′- and 3′-UTRs or conserved 8-nt sequences at both the 5′- and 3′-CYC motifs (Fig. 2 and Table 1). Because of the lack of charges in the PNA backbone, cellular uptake of PNA by passive diffusion through lipid membranes is very slow (Wittung et al., 1995). We therefore conjugated the PNAs at the N-terminus to an arginine-rich cell-penetrating peptide, HIV-1 $Tat_{57–49}$ (N-RRRQRRKKR-C) (Wender et al., 2000) for efficient delivery into cells. An unrelated PNA targeting the hepatitis C virus (HCV) 3′-end conserved sequence, the X-RNA recognized by HCV RdRp for minus-strand RNA synthesis (Oh et al., 2000), was used as a negative control. BHK-21 cells were treated with 10 μM of each Tat–PNA conjugate after JEV infection at an MOI of 0.05. Two days later, culture supernatants were harvested and titers of infectious virus were determined by viral plaque assays. As shown in Fig. 3, the PNAs targeting the 5′-UTR showed approximately 20% (J5U2) to 60% (J5U1) inhibition of JEV production compared to a non-PNA-treated control or the HCV-X-treated sample. The two PNAs J5C1 and J5C2, targeting the 5′-CYC motif, decreased the virus titer by approximately 40% and 70%, respectively. Unexpectedly, J5C1, targeting the 8-nt conserved sequence at the 5′-CYC, was less effective than

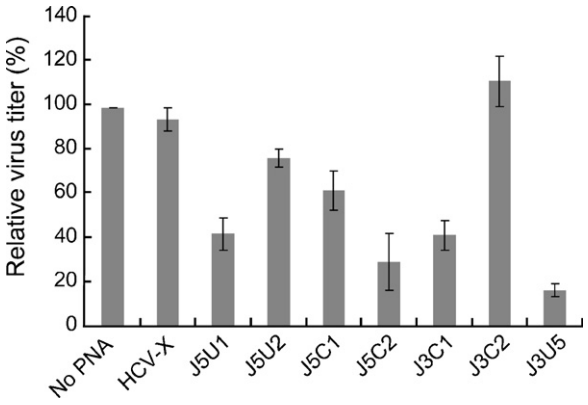

Fig. 3. Effect of various 15-mer Tat–PNA conjugates on JEV proliferation. BHK-21 cells were infected with JEV at an MOI of 0.05 and treated with each of the indicated PNAs (10 μM). At 48 h post-infection, supernatants were harvested, and JEV titers were determined by viral plaque assays. The relative plaque forming units are shown as a percentage of virus titer from untreated cells (no PNA). Error bars indicate the standard error of the mean of three independent experiments.

J5C2, which targeted the genome just downstream of the conserved sequence. PNA J3C1, targeting the 3′-CYC motif, showed ~60% inhibition, but PNA J3C2, designed to target 2-nt upstream of J3C1, did not reduce JEV titer, suggesting that the antisense activity of the PNA seemed to be affected by the *in vivo* accessibility of targets. Among the 15-mer PNAs tested, PNA J3U5, targeting the unpaired region forming a closed loop within the conserved SL structure of the 3′-UTR, was most effective in suppressing virus replication, with >80% inhibition of virus titer at a concentration of 10 μM. The inhibition levels of both an unrelated PNA (HCV-X) and the non-PNA-treated control on JEV production were considerably lower than that of the targeted PNAs, suggesting that the inhibitory effect of the targeted PNAs was specific.

3.3. Suppression of viral replication by PNA J3U5 targeting a 3′-UTR loop region

We further characterized the antiviral effects of PNA J3U5, which showed the greatest inhibitory effect among the 15-mer PNAs targeting various *cis*-acting elements on the JEV genome. First, we wanted to verify the entry of the Tat–PNA conjugate into cells and to monitor the cellular distribution of the entered PNA. FAM-labeled PNA J3U4, a 13-mer derivative of J3U5, was added to BHK-21 cells at a final concentration of 2 μM. After incubation for 1 min at room temperature, the cells were washed immediately with PBS several times. After medium was added to the cells, live fluorescent cell images were observed in a fluorescence microscope. Remarkably, most of the cells incubated with the FAM-labeled J3U4 were fluorescence-positive (Fig. 4A), indicating that the Tat–PNA conjugate could efficiently penetrate cell membranes within minutes and localized in the cytosol and nucleus. Similar staining patterns were also observed in JEV-infected cells (data not shown).

We next assessed the cytotoxicity of the Tat-conjugated PNA J3U5 by using an MTT assay. BHK-21 cells were treated with increasing concentrations of PNA J3U5 (0–50 μM) for 48 h. As shown in Fig. 4B, PNA J3U5 showed no significant cytotoxicity up to a concentration of 10 μM. Cell viability, however, decreased by approximately 15% and 20% at a concentration of 20 μM and 50 μM, respectively (Fig. 4B). Finally, we investigated whether the inhibitory effect of the Tat–PNA conjugates on JEV production was accompanied by a decrease of viral genome copy and protein levels. JEV-infected BHK-21 cells were treated with increasing concentrations of PNA J3U5 (0–10 μM), and intracellular viral genome copy number and viral protein levels were estimated by real-time quantitative RT-PCR and Western blot analyses, respectively, at 2 days PI. PNA treatment decreased intracellular JEV RNA levels in a dose-dependent manner, with almost 95% inhibition with 10 μM of J3U5 (Fig. 4C). Consequently, both viral envelope (Env) and NS5 protein levels also decreased (Fig. 4D). Altogether, these results

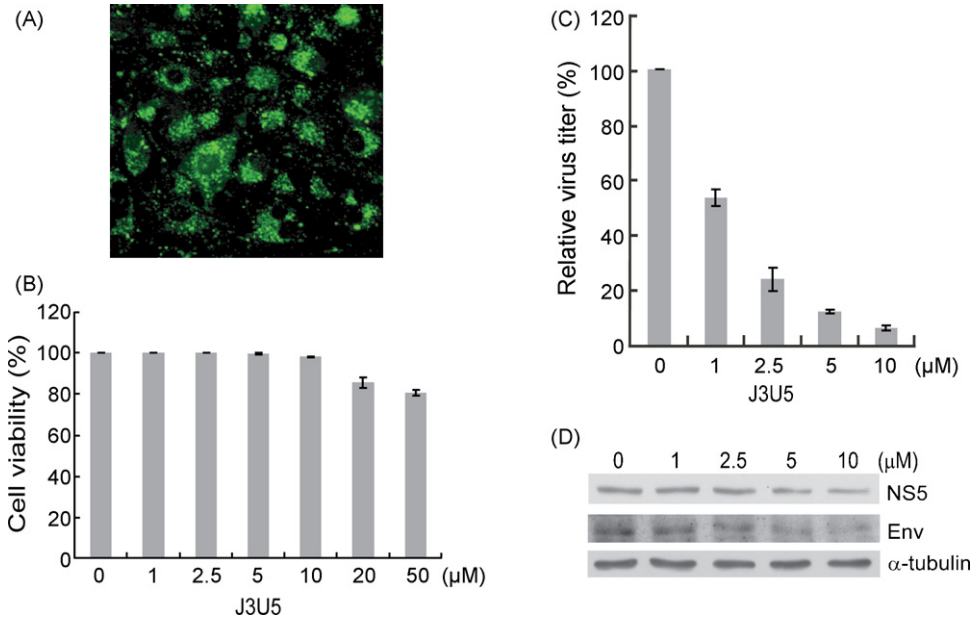

Fig. 4. Reduction of intracellular viral genome and protein levels by the delivery of a Tat–PNA conjugate. (A) Cellular delivery of PNA by covalent conjugation with a Tat_{57-49} peptide. BHK-21 cells were incubated with the FAM-labeled PNA J3U4 (2 μM). After 1 min of incubation, followed by several quick washes, cells were observed in a fluorescence microscope. (B) Cytotoxicity of Tat-conjugated PNA. BHK-21 cells in a 96-well plate were treated with various concentrations of PNA J3U5. Three independent MTT assays were performed in triplicate. Data are mean (% of control mean) ± S.E. of three independent experiments. (C and D) Dose-dependent inhibition of JEV replication by PNA J3U5. JEV-infected BHK-21 cells were treated with the indicated concentrations of J3U5 for 48 h. (C) Intracellular JEV genome copy numbers were quantified by real-time RT-PCR and expressed as percent of untreated control. The RT-PCR was performed with triplicates and data shown are the mean ± S.D. of three independent experiments. (D) Levels of NS5 and envelope (Env) proteins were determined by immunoblotting cell lysates (50 μg) with antibodies specific for the indicated proteins. An anti-α-tubulin antibody was used as an internal loading control.

demonstrate that the Tat–PNA conjugate effectively suppressed JEV proliferation by decreasing the levels of both viral RNA and proteins in a dose-dependent manner.

3.4. Effect of various PNAs targeting the 3′-UTR top loop region on JEV production

After finding that PNA J3U5, targeting the top of the 3′-UTR loop structure, effectively inhibits virus proliferation, we sought to further map the site where the PNA can access the stem loop more efficiently and possibly exert a greater antiviral activity. We designed various PNAs (PNA J3U1, 13-mer; PNA J3U2, 15-mer; PNA J3U3, 17-mer; PNA J3U4, 13-mer; PNA J3U5, 15-mer; and PNA J3U6, 17-mer) targeting different sites spanning the unpaired loop region of the 3′-UTR (Fig. 2) and tested their antiviral activities. JEV-infected BHK-21 cells were treated with each of the PNAs (10 μM) and culture supernatants were harvested for plaque assays at 48 h PI. Among the six PNAs tested, 17-mer PNA J3U6 exhibited the greatest antiviral activity (Fig. 5A). Notably, J3U4 and J3U5, targeting the portion of the loop region that does not include the penta-nucleotide motif conserved in all mosquito-borne flaviviruses (Figs. 1 and 2) (Hahn et al., 1987), also showed an inhibitory effect comparable to that of PNAs J3U1, J3U2, and J3U3, all of which target the region that includes the penta-nucleotide motif. This result suggested an important role of the region downstream of the penta-nucleotide motif in virus amplification.

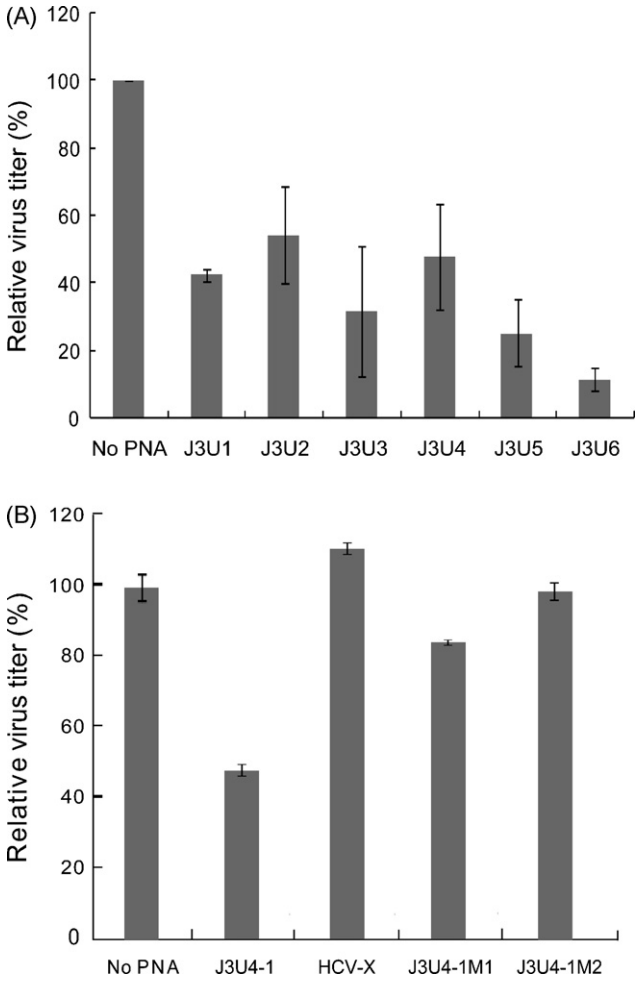

Fig. 5. Position-dependent and sequence-specific inhibition of JEV production by Tat–PNA conjugates targeting the top of the 3′-UTR loop structure. (A) JEV-infected BHK-21 cells were treated with each of the indicated PNAs (10 μM) targeting different sites at the top of the 3′-UTR loop structure. Culture supernatants were collected at 48 h PI and subjected to plaque assays as in Fig. 3. (B) Sequence-specific inhibition of JEV production by the 13-mer J3U4 targeting the loop region, not including the penta-nucleotide motif. Plaque assays were performed using the supernatant from JEV-infected BHK-21 cells after treatment with the indicated PNAs as in Fig. 3.

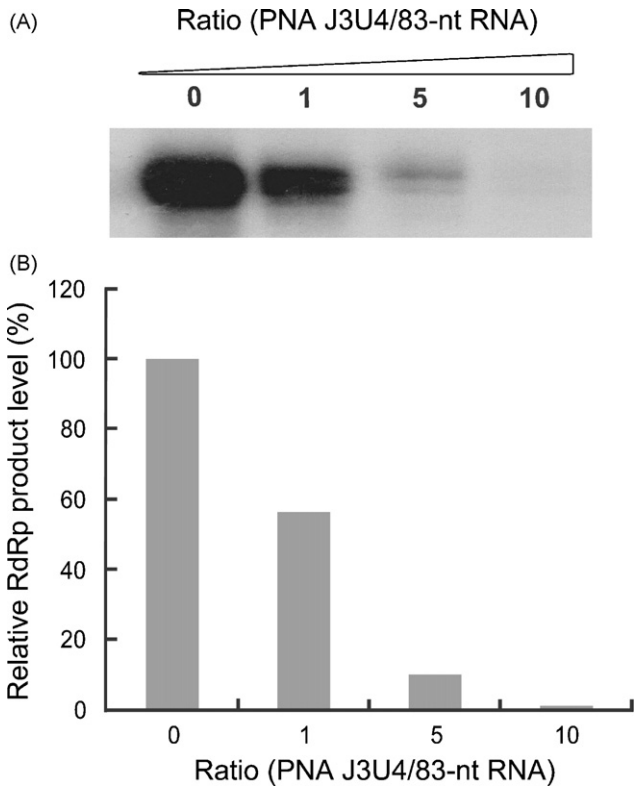

Fig. 6. *In vitro* inhibition of JEV RNA synthesis by PNA J3U4 targeting the top of the 3′-UTR loop structure. *In vitro* RdRp assays were performed with the 3′-terminal 83-nt RNA as a template in the presence of the indicated increasing concentrations of J3U4. (A) Labeled RdRp products were resolved on an 8 M urea–5% polyacrylamide gel, dried, and exposed to X-ray film. (B) Quantification of data in panel (A), showing the percentage of RdRp product level relative to the no PNA treatment control.

In order to further prove this possibility, we tested the anti-JEV activity of the 13-mer PNA J3U4 and two different mismatched derivatives of J3U4. The one-nucleotide mismatched PNA J3U4-1M1 and the two-nucleotide mismatched PNA J3U4-1M2 had little or no effect on virus production (Fig. 5B). As expected, the unrelated PNA targeting HCV-X (Oh et al., 2000) did not reduce JEV production. These results clearly demonstrated that the PNA-mediated inhibition of virus production appears to be quite target sequence-specific. Important roles of the non-penta-nucleotide region at the 3′-end loop region in virus RNA replication were demonstrated by *in vitro* RdRp assays showing that the PNA J3U4 inhibited RNA synthesis from the 3′-UTR 83-nt RNA template (Fig. 6), which was previously identified as a minimal RNA template required for the initiation of minus-strand RNA synthesis *in vitro* (Kim et al., 2007).

3.5. Mapping of the c5′-UTR minimal domain required for plus-strand JEV RNA synthesis

During the plus-strand RNA virus replication cycle, genomic RNA serves as a template for the synthesis of minus-strand RNA, and the minus-strand RNA serves as a template for the synthesis of plus-strand genomic RNA. Therefore, the c5′-UTR, or reverse complement of the 5′-UTR, at the 3′-end of the minus-strand viral RNA is likely to form the site for the initiation of plus-strand synthesis. Indeed, our previous work showed that the c5′-UTR serves as an RNA template for RNA synthesis *in vitro* (Kim et al., 2007). In the present study, we mapped the minimal *cis*-acting RNA region

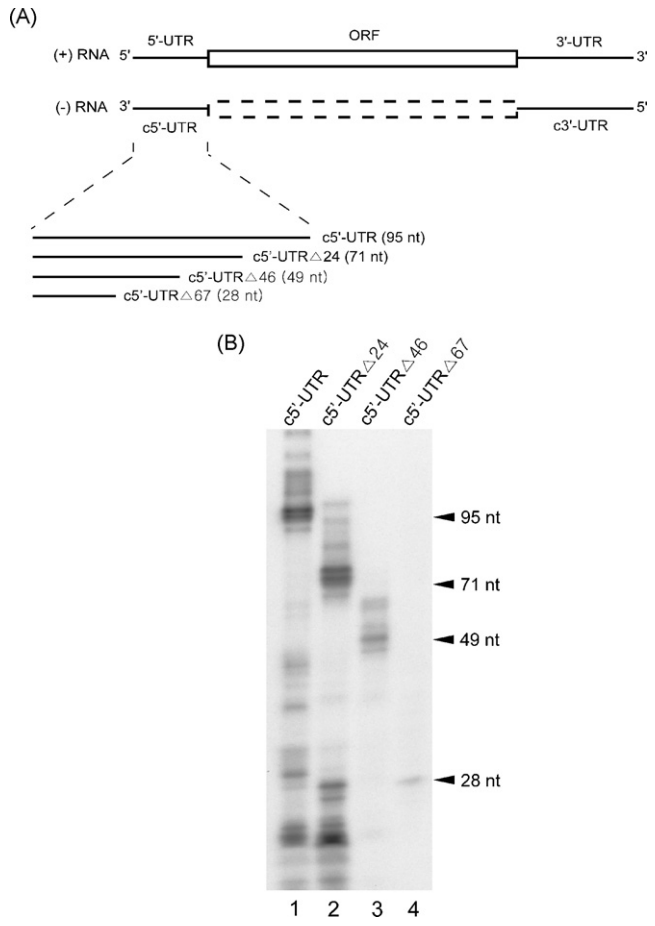

Fig. 7. Mapping of the minimal RNA template required for the synthesis of plus-strand JEV RNA. (A) Schematic representation of the RNA templates used for RdRp assays. Various JEV deletion derivatives of the c5′-UTR, which is complementary to the 5′-UTR, were used to map a minimal *cis*-acting RNA template required for plus-strand RNA synthesis. The RNA templates were obtained by *in vitro* transcription using the T7 RNA polymerase. Expected template sizes are shown in parentheses. (B) *De novo* RNA synthesis using the c5′-UTR and its deletion derivatives. *In vitro* RdRp activity assays were performed and the labeled RdRp products were analyzed as in Fig. 6A.

within the 95-nt c5′-UTR that is required for JEV NS5 RdRp to initiate plus-strand RNA synthesis. *In vitro* RdRp activity assays with serial deletion derivatives of c5′-UTR (c5′-UTRΔ24, c5′-UTRΔ46, and c5′-UTRΔ67, Fig. 7A) showed that viral RdRp required as little as 28-nt from the 3′-end for RNA synthesis initiation (Fig. 7B). Therefore, the NS5 protein can recognize the c5′-UTR for plus-strand RNA synthesis, with the 3′-end 28-nt RNA as a minimal template, indicating that the c5′-UTR can be a target of PNAs that potentially block binding of viral RNA polymerase.

3.6. Evaluation of the anti-JEV activity of PNAs targeting the c5′-UTR

Despite its essential role in JEV infection, the minus-strand of the JEV genome has not yet been subjected to extensive molecular characterization, and in comparison with other flavivirus genomes and proteomes, it remains relatively unexplored as a target for antiviral therapy. We designed four PNAs targeting various single-stranded loop regions at the c5′-UTR (Fig. 8A) and tested their ability to bind to the c5′-UTR. Various untagged PNAs [fJ3U1(−), fJ3U2(−), fJ3U3(−), and fJ3U4(−)] and an unrelated PNA fJ3U4 targeting the JEV plus-strand 3′-UTR were used in gel electrophoretic mobility shift assays (EMSA) using the ^{32}P-labeled c5′-UTR as a probe. Each PNA (500 fmol) was incubated with the probe (50 fmol), and the RNA–PNA complexes were analyzed by electrophoresis on a 5% non-denaturing polyacrylamide gel. As shown in Fig. 8B, a distinct shift in the mobility of the labeled probe was observed for fJ3U1(−), fJ3U3(−), and fJ3U4(−). In contrast, no RNA–PNA complex was formed with the fJ3U2(−) (lane 3), which was likely due to steric hindrance by RNA structures. As expected, no complex was formed with the non-specific, unrelated PNA fJ3U4 (lane 6).

In vitro RdRp activity assays were then performed to investigate whether the PNAs block RNA synthesis initiation. RdRp reactions were set up with the c5′-UTR RNA template (10 pmol) in the presence of each PNA (10-fold molar excess over the RNA template). The radioisotope-labeled products, after heat denaturation and quick chilling on ice, were analyzed by 8 M urea–8% PAGE for autoradiography. As shown in Fig. 8C, fJ3U1(−), fJ3U3(−), and fJ3U4(−), which bound the target in EMSA (Fig. 8B), inhibited RNA synthesis initiation to various degrees, with the fJ3U3(−) being the most effective at blocking RNA synthesis. In contrast, fJ3U2(−), which could not recognize the target in EMSA, showed no significant inhibitory effect.

We next explored the feasibility of targeting cell-penetrating peptide (CPP)–PNAs to RNA elements within the terminal region of JEV minus-strand RNA. JEV-infected BHK-21 cells were treated with 10 μM Tat-conjugated PNA J3U3(−) or PNA J3U4(−), which effectively inhibited RNA synthesis *in vitro* (Fig. 8C), and plaque assays were performed using the culture supernatants harvested at 2 days PI. PNA J3U3(−) and J3U4(−) reduced virus titer by 43% and 28%, respectively. The antiviral activity of those two PNAs, however, was less effective than that of PNA J3U6, which targeted the top of the 3′-UTR loop structure (Fig. 8D).

3.7. PNA J3U3(−) blocks the binding of viral RNA polymerase to the c5′-UTR

The results described above suggested that a sequence-specific PNA might inhibit RNA synthesis by blocking the JEV RdRp NS5 protein–RNA template interaction. To test this possibility, we examined whether JEV NS5 binds the c5′-UTR using EMSA. Various concentrations of purified NS5 protein (50 fmol to 5 pmol) were incubated with the ^{32}P-labeled c5′-UTR probe (50 fmol), and the reaction mixtures were then resolved on a 5% non-denaturing polyacrylamide gel for autoradiography. As shown in Fig. 9A, a distinct shift in the mobility of the probe was observed at as low as a 10-fold molar excess of NS5 protein over the probe, indicating that the NS5 was indeed able to bind the c5′-UTR of the JEV genome. A higher concentration of NS5 appeared to result in dimerization or oligomerization of NS5, or binding at multiple sites on the template (lane 8). We then investigated whether c5′-UTR-targeting PNA fJ3U3(−), which inhibited RNA synthesis most effectively (Fig. 8C), can block the interaction between NS5 and the RNA template. Various concentrations of PNA fJ3U3(−) (500 fmol, 2.5 pmol, and 5 pmol) were added to the probe (50 fmol) for competition with NS5 (500 fmol). As shown in Fig. 9B, competitive EMSA revealed that the amount of RNA–NS5 complex (lane 2) decreased with increasing fJ3U3(−) concentration, and consequent increase of the amount of the RNA–PNA complex (lanes 4 and 5). This result suggested that PNA fJ3U3(−) inhibited RNA synthesis by blocking the NS5–RNA template interaction.

4. Discussion

Despite an effort to understand JEV molecular biology, immunology, and pathology, little progress has been made in the area of therapeutics, and currently no effective antiviral therapy is available for the treatment of JEV infection (Leyssen et al., 2003). In this

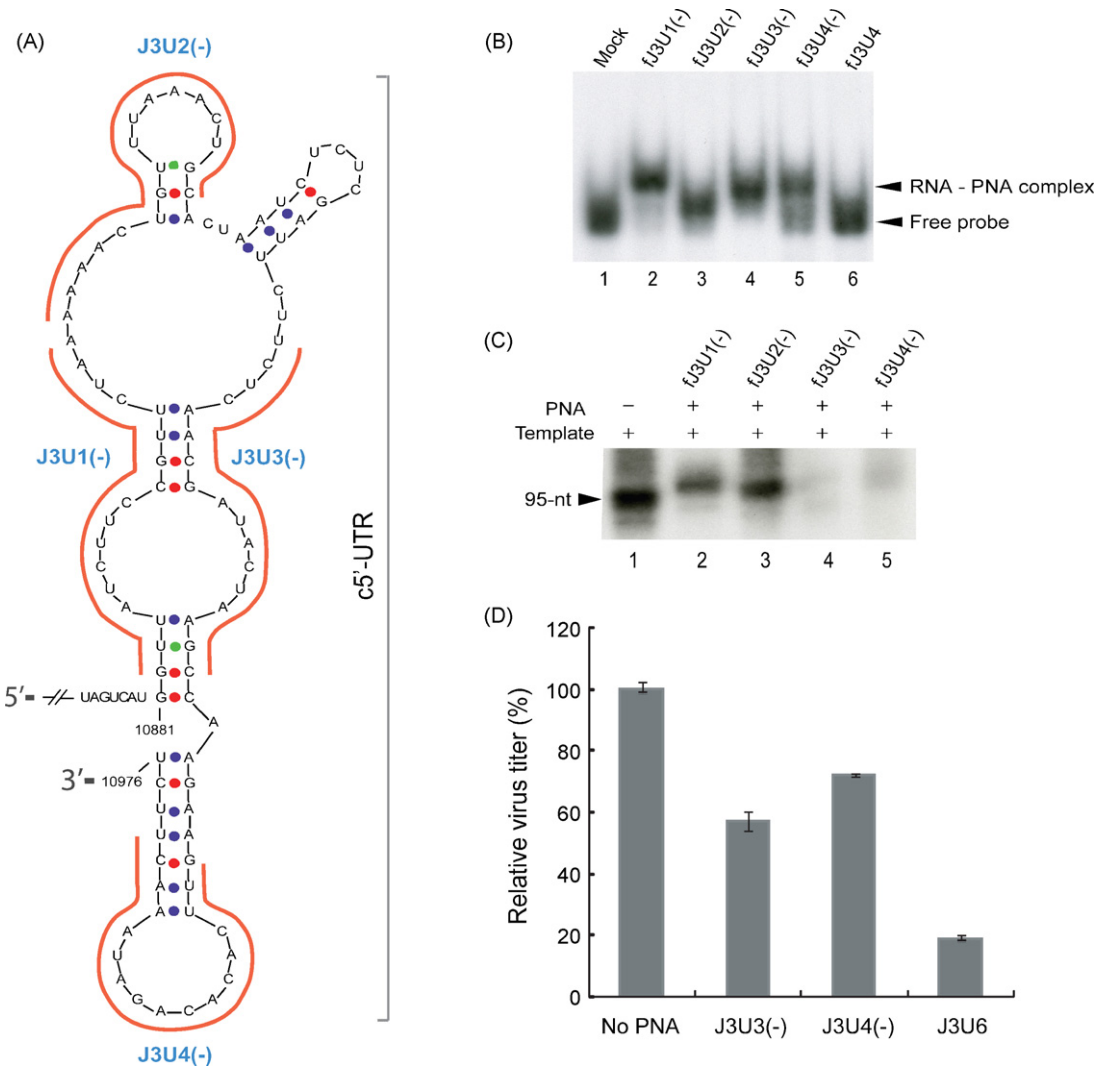

Fig. 8. Anti-JEV activity of the PNAs targeting the 3′-end stem-loop regions of the c5′-UTR. (A) The RNA secondary structure, predicted using the Mfold program, for the 3′-end region of JEV minus-strand RNA is shown to display the sites where four different antisense Tat–PNAs target. Individual Tat–PNAs are indicated by their names and targeted regions with red lines. (B) ^{32}P-labeled 95-nt c5′-UTR RNA (50 fmol) was incubated with various PNAs (50 fmol) as indicated above the autoradiogram. The mixtures were then analyzed on a 5% non-denaturing polyacrylamide gel. The gel was dried and exposed to X-ray film. Lane 1, free probe; lanes 2–5, non-Tat-tagged PNAs targeting the 3′-end region of the JEV minus-strand RNA; lane 6, non-Tat-tagged J3U4 targeting the 3′-UTR. (C) Inhibition of JEV RNA synthesis by PNAs targeting the 3′-end region of JEV minus-strand RNA. *In vitro* RdRp assays were performed with the purified NS5 and minus-strand 3′-end 95-nt RNA template in the presence of PNAs targeting different loop regions of the template. RdRp products were resolved by 8 M urea–8% PAGE for autoradiography. (D) Inhibition of JEV propagation by PNA J3U3(−) and J3U4(−). BHK-21 cells were infected with JEV at an MOI of 0.05 and treated with the indicated PNAs (10 μM). Plaque assays were performed using the supernatants harvested at 48 h post-infection as in Fig. 3.

study, we demonstrated that various antisense PNAs targeting *cis*-acting elements on the plus- and minus-strands of JEV RNA had antiviral activity.

The flavivirus 3′-terminal sequence has been thermodynamically predicted and experimentally demonstrated to fold into a stable secondary structure. The conformation and stability of this structure are conserved among divergent flaviviruses even though only short regions of the sequence are conserved (Proutski et al., 1997; Rauscher et al., 1997; Markoff, 2003). Deletion and mutation analyses of the 3′-terminal SL structures of flaviviruses revealed that this conserved RNA structure is critical for RNA replication (Khromykh and Westaway, 1997; Zeng et al., 1998; Proutski et al., 1999). In this study, we showed that blocking the top of the 3′-UTR loop structure with a PNA could effectively suppress virus propagation. One of the six different PNAs targeting this region, 17-mer J3U6, exhibited the greatest anti-JEV activity. Its shorter derivative, 13-mer PNA J3U4, targeting the site not encompassing the conserved penta-nucleotide region on this loop, also was shown to reduce virus titer. The J3U4 PNA was able to inhibit RNA synthesis initiation *in vitro*, as demonstrated by RdRp assays with the 3′-end 83-nt RNA, a minimal template for the initiation of minus-strand RNA synthesis (Kim et al., 2007), suggesting that the top loop region excluding the conserved penta-nucleotides carries an essential RNA element recognized by viral RdRp. Previously, the 3′-UTR region of the WNV genome was shown to interact with cellular proteins with molecular masses of 52 kDa, 84 kDa, and 105 kDa (Blackwell and Brinton, 1995). The 52-kDa protein was identified as eukaryotic elongation factor 1α (EF-1α), and the overall structure of the 3′-SL was demonstrated to be important for the binding of EF-1α to facilitate viral minus-strand RNA synthesis (Blackwell and Brinton, 1997; Davis et al., 2007). The JEV and WNV 3′-SLs were very conserved and a similar molecular mass protein, which has not been yet identified, was also found to bind JEV 3′-SL structure by UV-induced crosslinking experiments (Ta and Vrati, 2000). Therefore, an alternative possible explanation for the inhibition of virus production by the top loop-targeting PNAs is that the PNAs block the

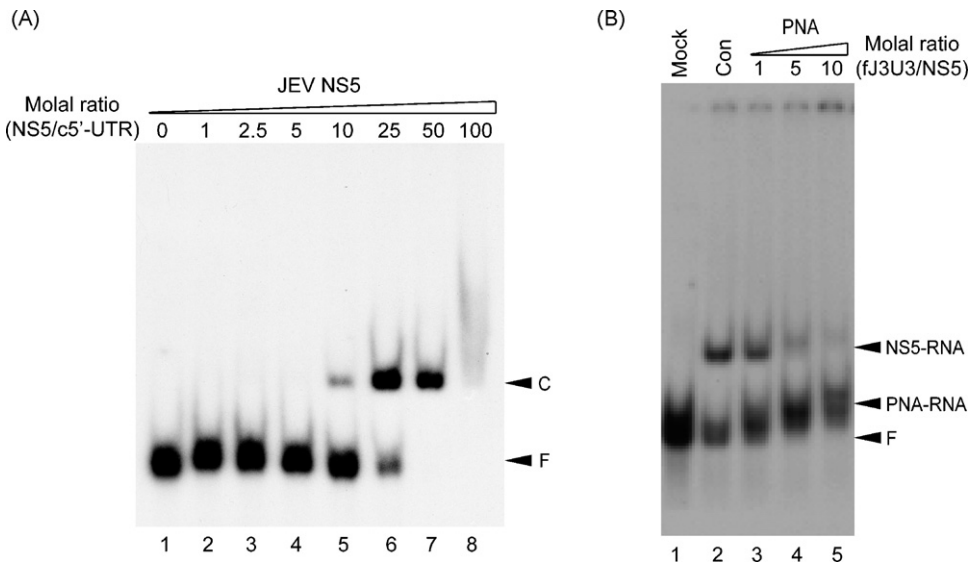

Fig. 9. Inhibition of the interaction between NS5 and the c5′-UTR by PNA fJ3U3(−). (A) EMSA analysis with the c5′-UTR probe and JEV NS5 RdRp. The ^{32}P-labeled 95-nt c5′-UTR (50 fmol) was incubated with increasing amounts of NS5 protein. Lane 1, free probe; lanes 2, 3, 4, 5, 6, 7, and 8 contained 50 fmol, 125 fmol, 250 fmol, 500 fmol, 1.25 pmol, 2.5 pmol, and 5 pmol of NS5 protein, respectively. The reaction products were analyzed on a 5% non-denaturing polyacrylamide gel. The protein–RNA complex (C) and free probe (F) are indicated with arrowheads. (B) Competition between the fJ3U3(−) PNA and JEV NS5 for binding to the c5′-UTR. ^{32}P-labeled c5′-UTR (50 fmol) was incubated with NS5 protein (500 fmol) in the absence or presence of increasing amounts of unlabeled competitor fJ3U3(−). Lane 1, free probe (Mock); lane 2, no PNA (Con). Lanes 3, 4, and 5 contained 500 fmol, 2.5 pmol, and 5 pmol of fJ3U3 PNA, respectively. The reaction mixtures were analyzed as in (A). The protein–RNA complex (NS5–RNA), PNA–RNA complex (PNA–RNA), and free probe (F) are indicated with arrowheads.

binding of host factor(s) required for RNA synthesis or viral genome translation.

Like the 3′-UTR, the 3′-terminal region of minus-strand JEV RNA or the c5′-UTR also is thought to be recognized by viral RNA polymerase for plus-strand RNA synthesis. Among the four PNAs designed to target the c5′-UTR, two PNAs, J3U3(−) and J3U4(−), inhibited RNA synthesis most effectively *in vitro* as demonstrated by RdRp assays. PNA J3U1(−) bound to the target as efficiently as J3U3(−) and J3U4(−) did; it was less effective in inhibiting RNA synthesis by purified JEV RdRp, suggesting that targets of J3U3(−) and J3U4(−) might be the binding sites for the polymerase to initiate minus-strand RNA synthesis. Alternatively, JEV RdRp might be too processive to be blocked by J3U1(−) bound far upstream of the 3′-end of the template. Considering that the c5′-UTR is a better RNA template than the 3′-UTR template for RNA synthesis *in vitro* (Kim et al., 2007), and that plus-strand RNA synthesis is 10–100 times more efficient than the minus-strand RNA synthesis in virus-infected cells (Chambers et al., 1990), PNAs targeting the c5′-UTR would have reduced virus titer more effectively. However, PNA J3U3(−), which showed the greatest inhibitory potency, was less effective in cell culture than J3U6, which targets the 3′-UTR. This might be due to the difficulty of the PNA to access minus-strand RNAs, considering the fact that they form a double-stranded replication intermediate with excess copies of plus-strand viral genome in infected cells.

The 5′-UTR-targeting PNAs J5U1 and J5U2, which were designed to bind single-strand loop regions upstream of the translation initiation site, also displayed antiviral activity. PNA J5U1, targeting an internal loop of one single U at the 5′-end, and two Us at the 3′ strand of the stem, inhibited JEV production more effectively than J5U2. We found that this sequence is well-conserved among JEV, MVEV, WNV, and YFV, and the structure is well-conserved among JEV, DENV, and YFV (Thurner et al., 2004). The inhibition observed by using the 5′-UTR-targeted PNAs is likely due to the blocking of translation elongation, as is seen with other PNAs that reduce expression of cellular capped messenger RNAs (Lundin et al., 2006). We also demonstrated that JEV genome cyclization motifs are important *cis*-acting elements that can be targeted by antisense PNAs. A part of the 3′-CYC motif on the JEV genome has a conserved 8-nt sequence complementary to the conserved sequence in the region encoding the capsid protein. We confirmed the interactions between the 5′- and 3′-CYC motifs of the JEV genome by EMSA, as expected (data not shown). The PNAs targeting the 5′- and 3′-CYC motifs of the JEV genome inhibited virus production to various degrees. Similarly, other groups have also demonstrated antiviral activities using antisense morpholino oligomers targeting the 3′-CYC motif of DENV and WNV (Deas et al., 2005; Kinney et al., 2005; Holden et al., 2006). Interestingly, even though PNAs J3C1 and J3C2, targeting sites within 3′-CYC, differ from each other in only 2 nt of the targeting sequence, J3C2 exhibited almost no inhibitory effects, suggesting that the *in vivo* structure of this target might be different from those predicted *in vitro*, formed in the absence of any interacting viral and/or cellular proteins. Furthermore, J5C2, targeting a region downstream of the 8-nt conserved sequence within the 5′-CYC motif, was unexpectedly a better inhibitor than J5C1, which fully encompassed the 8-nt conserved sequence. These results underscore the fact that it is difficult to predict the optimal *in vivo* antisense-targeting sites because they might be shielded either by complicated tertiary RNA structures or by cellular proteins or viral protein in infected cells. However, CPP–PNAs are still a useful tool for the *in vivo* probing of accessible sites for antisense agents in the milieu of cellular and viral proteins.

Because of the lack of charges in the backbone of PNAs, some type of assisted delivery is required for efficient cellular uptake of PNAs (Lundin et al., 2006). In the present study, we used an arginine-rich HIV-1 Tat peptide that was previously shown to efficiently penetrate cell membranes (Vives et al., 1997; Turner et al., 2005). Live cell image analysis revealed that the Tat peptide-conjugated PNA was delivered into cells after simply incubating it with cells for a few minutes. Assuming that JEV replication occurs within a membranous structure, as demonstrated for other flaviviruses (Lindenbach and Rice, 2003; Aizaki et al., 2004; Miller et al., 2007), the PNAs targeting the 3′-end regions of the plus- and minus-strand viral RNAs to block the binding of viral RNA polymerase or cellular proteins involved in viral RNA replication need to penetrate the membranous structures in JEV-infected cells (Uchil and Satchidanandam,

2003). It appears that Tat–PNA conjugates can invade such structures to recognize the targets probably within highly structured RNAs, allowing the PNA to function as an antisense agent. Recently, antisense peptide-conjugated PMOs have been used successfully to inhibit other flaviviruses such as DENV (Stein and Shi, 2008) and WNV (Deas et al., 2007) in animal models. For neurotropic JEV (Tyler and Nathanson, 2001), one critical hurdle to overcome prior to using anti-JEV PNAs *in vivo* is how to deliver PNAs into brain tissues so that they might exert proper antiviral effects. A previous study successfully demonstrated that even PNA alone, administered by intraperitoneal injection, crosses the blood–brain barrier (BBB) (Tyler et al., 1999). Furthermore, even Tat-fused protein was successfully delivered to brain (Schwarze et al., 1999). Nevertheless, more *in vivo* experimentation will be needed to evaluate whether Tat–PNA conjugates can show substantial antiviral efficacy by crossing the BBB. Furthermore, *in vivo* toxicity of Tat- or other CPP-conjugated PNA and immune responses against PNA need to be tested.

In summary, we demonstrated the anti-JEV activities of various PNAs designed to block critical RNA–protein or RNA–RNA interactions involved in viral RNA synthesis and/or translation. Our results underscore the usefulness of CPP–PNAs as a tool for mapping *in vivo* accessible targets for antisense agents and for targeting both plus- and minus-strand viral RNAs, which might be protected by membranous structures surrounding viral RNA replicase complexes. The newly identified antisense targets for JEV are conserved in sequence or structure and thus warrant testing as antiviral therapies in other clinically important flaviviruses.

Acknowledgements

This work was supported by the Basic Research Program of the Korea Science and Engineering Foundation (RO1-2004-000-10382-0) and by a Korea Research Foundation Grant (KRF-2004-C00148) funded by the Korean Government. JSY, CMK, and JHK were supported in part by the BK21 Program of the Korean Ministry of Education, Science, and Technology.

References

Aizaki, H., Lee, K.J., Sung, V.M., Ishiko, H., Lai, M.M., 2004. Characterization of the hepatitis C virus RNA replication complex associated with lipid rafts. Virology 324, 450–461.

Blackwell, J.L., Brinton, M.A., 1995. BHK cell proteins that bind to the 3′ stem-loop structure of the West Nile virus genome RNA. J. Virol. 69, 5650–5658.

Blackwell, J.L., Brinton, M.A., 1997. Translation elongation factor-1 alpha interacts with the 3′ stem-loop region of West Nile virus genomic RNA. J. Virol. 71, 6433–6444.

Brinton, M.A., Dispoto, J.H., 1988. Sequence and secondary structure analysis of the 5′-terminal region of flavivirus genome RNA. Virology 162, 290–299.

Cahour, A., Pletnev, A., Vazielle-Falcoz, M., Rosen, L., Lai, C.J., 1995. Growth-restricted dengue virus mutants containing deletions in the 5′ noncoding region of the RNA genome. Virology 207, 68–76.

Chambers, T.J., Hahn, C.S., Galler, R., Rice, C.M., 1990. Flavivirus genome organization, expression, and replication. Annu. Rev. Microbiol. 44, 649–688.

Davis, W.G., Blackwell, J.L., Shi, P.Y., Brinton, M.A., 2007. Interaction between the cellular protein eEF1A and the 3′-terminal stem-loop of West Nile virus genomic RNA facilitates viral minus-strand RNA synthesis. J. Virol. 81, 10172–10187.

Deas, T.S., Bennett, C.J., Jones, S.A., Tilgner, M., Ren, P., Behr, M.J., Stein, D.A., Iversen, P.L., Kramer, L.D., Bernard, K.A., Shi, P.Y., 2007. In vitro resistance selection and in vivo efficacy of morpholino oligomers against West Nile virus. Antimicrob. Agents Chemother. 51, 2470–2482.

Deas, T.S., Binduga-Gajewska, I., Tilgner, M., Ren, P., Stein, D.A., Moulton, H.M., Iversen, P.L., Kauffman, E.B., Kramer, L.D., Shi, P.Y., 2005. Inhibition of flavivirus infections by antisense oligomers specifically suppressing viral translation and RNA replication. J. Virol. 79, 4599–4609.

Decker, C.J., Parker, R., 1995. Diversity of cytoplasmic functions for the 3′ untranslated region of eukaryotic transcripts. Curr. Opin. Cell Biol. 7, 386–392.

Dreher, T.W., 1999. Functions of the 3′-untranslated regions of positive strand RNA viral genomes. Annu. Rev. Phytopathol. 37, 151–174.

Hahn, C.S., Hahn, Y.S., Rice, C.M., Lee, E., Dalgarno, L., Strauss, E.G., Strauss, J.H., 1987. Conserved elements in the 3′ untranslated region of flavivirus RNAs and potential cyclization sequences. J. Mol. Biol. 198, 33–41.

Holden, K.L., Stein, D.A., Pierson, T.C., Ahmed, A.A., Clyde, K., Iversen, P.L., Harris, E., 2006. Inhibition of dengue virus translation and RNA synthesis by a morpholino oligomer targeted to the top of the terminal 3′ stem-loop structure. Virology 344, 439–452.

Khromykh, A.A., Meka, H., Guyatt, K.J., Westaway, E.G., 2001. Essential role of cyclization sequences in flavivirus RNA replication. J. Virol. 75, 6719–6728.

Khromykh, A.A., Westaway, E.G., 1997. Subgenomic replicons of the flavivirus Kunjin: construction and applications. J. Virol. 71, 1497–1505.

Kim, S.J., Kim, J.H., Kim, Y.G., Lim, H.S., Oh, J.W., 2004. Protein kinase C-related kinase 2 regulates hepatitis C virus RNA polymerase function by phosphorylation. J. Biol. Chem. 279, 50031–50041.

Kim, Y.G., Yoo, J.S., Kim, J.H., Kim, C.M., Oh, J.W., 2007. Biochemical characterization of a recombinant Japanese encephalitis virus RNA-dependent RNA polymerase. BMC Mol. Biol. 8, 59.

Kinney, R.M., Huang, C.Y., Rose, B.C., Kroeker, A.D., Dreher, T.W., Iversen, P.L., Stein, D.A., 2005. Inhibition of dengue virus serotypes 1 to 4 in Vero cell cultures with morpholino oligomers. J. Virol. 79, 5116–5128.

Kumar, P., Lee, S.K., Shankar, P., Manjunath, N., 2006. A single siRNA suppresses fatal encephalitis induced by two different flaviviruses. PLoS Med. 3, e96.

Leyssen, P., Charlier, N., Paeshuyse, J., De Clercq, E., Neyts, J., 2003. Prospects for antiviral therapy. Adv. Virus Res. 61, 511–553.

Leyssen, P., De Clercq, E., Neyts, J., 2000. Perspectives for the treatment of infections with Flaviviridae. Clin. Microbiol. Rev. 13, 67–82.

Lindenbach, B.D., Rice, C.M., 2003. Molecular biology of flaviviruses. Adv. Virus Res. 59, 23–61.

Lundin, K.E., Good, L., Strömberg, R., Gräslund, A., Smith, C.I., 2006. Biological activity and biotechnological aspects of peptide nucleic acid. Adv. Genet. 56, 1–51.

Mackenzie, J.S., Gubler, D.J., Petersen, L.R., 2004. Emerging flaviviruses: the spread and resurgence of Japanese encephalitis, West Nile and dengue viruses. Nat. Med. 10, S98–109.

Markoff, L., 2003. 5′- and 3′-noncoding regions in flavivirus RNA. Adv. Virus Res. 59, 177–228.

Miller, S., Kastner, S., Krijnse-Locker, J., Bühler, S., Bartenschlager, R., 2007. The non-structural protein 4A of dengue virus is an integral membrane protein inducing membrane alterations in a 2K-regulated manner. J. Biol. Chem. 282, 8873–8882.

Nielsen, P.E., Egholm, M., Berg, R.H., Buchardt, O., 1991. Sequence-selective recognition of DNA by strand displacement with a thymine-substituted polyamide. Science 254, 1497–1500.

Oh, J.W., Sheu, G.T., Lai, M.M., 2000. Template requirement and initiation site selection by hepatitis C virus polymerase on a minimal viral RNA template. J. Biol. Chem. 275, 17710–17717.

Parida, M., Dash, P.K., Tripathi, N.K., Ambuj, Sannarangaiah, S., Saxena, P., Agarwal, S., Sahni, A.K., Singh, S.P., Rathi, A.K., Bhargava, R., Abhyankar, A., Verma, S.K., Rao, P.V., Sekhar, K., 2006. Japanese encephalitis outbreak, India, 2005. Emerg. Infect. Dis. 12, 1427–1430.

Proutski, V., Gould, E.A., Holmes, E.C., 1997. Secondary structure of the 3′ untranslated region of flaviviruses: similarities and differences. Nucleic Acids Res. 25, 1194–1202.

Proutski, V., Gritsun, T.S., Gould, E.A., Holmes, E.C., 1999. Biological consequences of deletions within the 3′-untranslated region of flaviviruses may be due to rearrangements of RNA secondary structure. Virus Res. 64, 107–123.

Rauscher, S., Flamm, C., Mandl, C.W., Heinz, F.X., Stadler, P.F., 1997. Secondary structure of the 3′-noncoding region of flavivirus genomes: comparative analysis of base pairing probabilities. RNA 3, 779–791.

Schwarze, S.R., Ho, A., Vocero-Akbani, A., Dowdy, S.F., 1999. In vivo protein transduction: delivery of a biologically active protein into the mouse. Science 285, 1569–1572.

Shi, P.Y., 2002. Strategies for the identification of inhibitors of West Nile virus and other flaviviruses. Curr. Opin. Investig. Drugs 3, 1567–1573.

Solomon, T., 2003. Recent advances in Japanese encephalitis. J. Neurovirol. 9, 274–283.

Spurgers, K.B., Sharkey, C.M., Warfield, K.L., Bavari, S., 2008. Oligonucleotide antiviral therapeutics: antisense and RNA interference for highly pathogenic RNA viruses. Antiviral Res. 78, 26–36.

Stein, D.A., Shi, P.Y., 2008. Nucleic acid-based inhibition of flavivirus infections. Front. Biosci. 13, 1385–1395.

Sumiyoshi, H., Mori, C., Fuke, I., Morita, K., Kuhara, S., Kondou, J., Kikuchi, Y., Nagamatu, H., Igarashi, A., 1987. Complete nucleotide sequence of the Japanese encephalitis virus genome RNA. Virology 161, 497–510.

Suzuki, T., Futaki, S., Niwa, M., Tanaka, S., Ueda, K., Sugiura, Y., 2002. Possible existence of common internalization mechanisms among arginine-rich peptides. J. Biol. Chem. 277, 2437–2443.

Ta, M., Vrati, S., 2000. Mov34 protein from mouse brain interacts with the 3′ noncoding region of Japanese encephalitis virus. J. Virol. 74, 5108–5115.

Thurner, C., Witwer, C., Hofacker, I.L., Stadler, P.F., 2004. Conserved RNA secondary structures in Flaviviridae genomes. J. Gen. Virol. 85, 1113–1124.

Tsai, T.F., 2000. New initiatives for the control of Japanese encephalitis by vaccination: minutes of a WHO/CVI meeting, Bangkok, Thailand, 13–15 October 1998. Vaccine 18 (Suppl. 2), 1–25.

Turner, J.J., Ivanova, G.D., Verbeure, B., Williams, D., Arzumanov, A.A., Abes, S., Lebleu, B., Gait, M.J., 2005. Cell-penetrating peptide conjugates of peptide nucleic acids (PNA) as inhibitors of HIV-1 Tat-dependent trans-activation in cells. Nucleic Acids Res. 33, 6837–6849.

Tyler, B.M., Jansen, K., McCormick, D.J., Douglas, C.L., Boules, M., Stewart, J.A., Zhao, L., Lacy, B., Cusack, B., Fauq, A., Richelson, E., 1999. Peptide nucleic acids targeted

to the neurotensin receptor and administered i.p. cross the blood–brain barrier and specifically reduce gene expression. Proc. Natl. Acad. Sci. U.S.A. 96, 7053–7058.
Tyler, K.N., Nathanson, N., 2001. Pathogenesis of viral infections. In: Fields, B.N., Knipe, D.M., Howley, P.M. (Eds.), Fields Virology, 4th ed. Lippincott/Williams & Wilkins, Philadelphia, PA, pp. 199–244.
Uchil, P.D., Satchidanandam, V., 2003. Characterization of RNA synthesis, replication mechanism, and in vitro RNA-dependent RNA polymerase activity of Japanese encephalitis virus. Virology 307, 358–371.
Vives, E., Brodin, P., Lebleu, B., 1997. A truncated HIV-1 Tat protein basic domain rapidly translocates through the plasma membrane and accumulates in the cell nucleus. J. Biol. Chem. 272, 16010–16017.
Wender, P.A., Mitchell, D.J., Pattabiraman, K., Pelkey, E.T., Steinman, L., Rothbard, J.B., 2000. The design, synthesis, and evaluation of molecules that enable or enhance cellular uptake: peptoid molecular transporters. Proc. Natl. Acad. Sci. U.S.A. 97, 13003–13008.
Wittung, P., Kajanus, J., Edwards, K., Haaima, G., Nielsen, P.E., Nordén, B., Malmström, B.G., 1995. Phospholipid membrane permeability of peptide nucleic acid. FEBS Lett. 375, 27–29.
You, S., Falgout, B., Markoff, L., Padmanabhan, R., 2001. In vitro RNA synthesis from exogenous dengue viral RNA templates requires long range interactions between 5′- and 3′-terminal regions that influence RNA structure. J. Biol. Chem. 276, 15581–15591.
Yun, S.I., Kim, S.Y., Rice, C.M., Lee, Y.M., 2003. Development and application of a reverse genetics system for Japanese encephalitis virus. J. Virol. 77, 6450–6465.
Zeng, L., Falgout, B., Markoff, L., 1998. Identification of specific nucleotide sequences within the conserved 3′-SL in the dengue type 2 virus genome required for replication. J. Virol. 72, 7510–7522.
Zhao, M., Weissleder, R., 2004. Intracellular cargo delivery using tat peptide and derivatives. Med. Res. Rev. 24, 1–12.
Zuker, M., 2003. Mfold web server for nucleic acid folding and hybridization prediction. Nucleic Acids Res. 31, 3406–3415.